Available online at www.sciencedirect.com
ScienceDirect
Ceramics International 35 (2009) 2061–2067
CERAMICS INTERNATIONAL
www.elsevier.com/locate/ceramint

Structure and enhanced properties of perovskite ferroelectric PNN–PZN–PMN–PZ–PT ceramics by Ni and Mg doping

Bee Keen Gan, Kui Yao *

*Institute of Materials Research and Engineering, A*STAR (Agency for Science, Technology and Research), 3 Research Link, 117602, Singapore*

Received 31 July 2008; received in revised form 7 October 2008; accepted 11 November 2008
Available online 9 December 2008

Abstract

Perovskite ferroelectric oxide ceramics of $0.1Pb(Ni_{1/3}Nb_{2/3})O_3$–$0.35Pb(Zn_{1/3}Nb_{2/3})O_3$–$0.15Pb(Mg_{1/3}Nb_{2/3})O_3$–$0.1PbZrO_3$–$0.3PbTiO_3$ (0.10PNN–0.35PZN–0.15PMN–0.10PZ–0.30PT) with excess MgO and NiO were investigated in this work. The effects of the excess MgO and NiO doping on the ceramic structure, density, dielectric, ferroelectric and piezoelectric properties were studied. The chemical states of nickel were examined using X-ray photoelectron spectroscopy (XPS). Both XPS experimental results and theoretical analyses on the basis of ionic packing indicated that the excess valence-two ions substituted the A-sites in the ABO_3 perovskite structure. By completely eliminating the pyrochlore phase and enhancing densification with the excess NiO and MgO, improved piezoelectric coefficient d_{33} up to 459 *pC/N*, higher ferroelectric remnant polarization and dielectric constant were demonstrated when sintered at temperature as low as 850–950 °C.

Keywords: A. Sintering; C. Ferroelectric properties; C. Piezoelectric properties; D. Perovskite

1. Introduction

Ferroelectric ceramics with a general formula of ABO_3, such as lead zirconate titanate (PZT), lead zinc niobate (PZN), lead magnesium niobate (PMN), lead nickel niobate (PNN), and lead titanate (PT) and their solid solutions are widely used for many different applications due to their ferroelectric and piezoelectric properties [1–3]. These ferroelectric ceramics require densification at sintering temperatures higher than 1200 °C in general. Recently, we [4] reported a ferroelectric solid solution $0.1Pb(Ni_{1/3}Nb_{2/3})O_3$–$0.35Pb(Zn_{1/3}Nb_{2/3})O_3$–$0.15Pb(Mg_{1/3}Nb_{2/3})O_3$–$0.1PbZrO_3$–$0.3PbTiO_3$ (0.10PNN–0.35PZN–0.15PMN–0.10PZ–0.30PT) with low sintering temperatures (850–950 °C). The low sintering temperature is highly desired as it enables the use of less expensive metals as electrodes [4–6]. Moreover, this composition containing relatively high concentration of PZN and PMN had a large piezoelectric coefficient (d_{33}) of 393 *pC/N* when sintered at 900 °C, although the composition is not at a morphortropic phase boundary (MPB). It has been reported in the literature [2,7–9] that a small amount of valence-two dopants such as MnO, NiO, FeO or MgO, can be added into lead-based perovskite ceramics in order to improve their microstructure and electrical properties, although the mechanisms for these dopants to stabilize the perovskite phase were not clearly explained.

Our study focuses on the impact of two effective dopants, NiO and MgO, on the structures and properties of our complex ceramic compositions which can be sintered at low temperature. The mechanisms of the lattice substitution of these valence-two ions in the perovskite structure for promoting perovskite phase and property improvement are also analyzed. A main composition of 0.10PNN–0.35PZN–0.15PMN–0.10PZ–0.30PT with relatively high PZN content was selected to report in this paper due to its large piezoelectric coefficient (d_{33}) when sintered at low temperature.

2. Experimental procedure

The undoped, and NiO or MgO doped ceramics of 0.1PNN–0.35PZN–0.15PMN–0.1PZ–0.3PT were fabricated via columbite approach. Three types of columbite precursors namely $NiNb_2O_6$ (NNO), $ZnNb_2O_6$ (ZNO) and $MgNb_2O_6$ (MNO) were prepared from various starting oxides, followed by mixing the

* Corresponding author. Tel.: +65 6874 5160; fax: +65 6872 0785.
E-mail address: k-yao@imre.a-star.edu.sg (K. Yao).

0272-8842/$34.00
doi:10.1016/j.ceramint.2008.11.015

obtained columbite precursors with other oxides, using the same method as described in the previous report [4]. In this investigation, the doped compositions had an excess of 1 mol% MgO or 2–4 mol% NiO. These powder mixtures were dried and calcined in the range of 800–850 °C. After calcination, 1 wt% of PbO and 5 wt% of polyvinyl alcohol (PVA) were added and the powder mixtures were then uniaxially pressed into small disks. The pressed ceramic disks were sintered from 800 to 950 °C in air for 1 h.

The oxidation states for nickel were characterized with X-ray photoelectron spectroscopy (XPS) (ESCALAB 220i XL, VG Scientific), calibrated with carbon peak. The crystalline phases were examined using X-ray diffraction (XRD) (Bruker D8 GADDS). The specimens' densities were measured based on Archimedes principle. The surface morphologies were inspected using field-emission scanning electron microscope (FESEM) (JSM-6700F, JEOL), after surface polishing followed by thermal etching in the range of 700–800 °C for 15 min.

For electrical properties measurement, silver electrodes were coated on both sides of the disks followed by firing at 520 °C for 10 min. Ferroelectric properties were examined using RT66A system (Radiant Technologies, US) and dielectric properties were measured using an impedance analyzer (HP4194A, Hewlett Packard) at room temperature. Piezoelectric coefficients d_{33} were obtained from a Piezo d_{33} Meter (Model ZJ-4B, Institute of Acoustics Chinese Academy of Science) in 24 h after poling under a field of 25 kV/cm at 125 °C in silicone oil for a duration of 20 min.

3. Results and discussion

3.1. Perovskite phase stabilization via A-site substitution by valence-two ions

ABO_3-perovskite phase was formed in all the examined samples. Fig. 1 shows the XPS spectra for Ni $2p_{3/2}$ peak for the undoped and 2–4 mol% Ni-doped ceramic disks sintered at 900 °C. As can be seen from this figure, the main binding energy peak for Ni $2p_{3/2}$ shifted to 1–1.5 eV higher when doped with 2 and 4 mol% of NiO, as compared to that of the undoped composition around 850 eV. For the 4 mol% doped composition, a smaller peak appeared at higher binding energy by 4–6 eV with respect to the main peak around 851 eV indicating a possible existence of Ni^{3+} in the composition [10,11]. This could also be due to satellite peaks of Ni^{2+} as a result of non-local screening as suggested by some reports [12–14]. At least, the higher binding energy in the case of Ni-doped composition is attributed to higher electronegativity for nickel cations, which indicates that excess Ni^{2+} cations enter the A-site of the perovskite structure.

The substitution mechanism of excess valence-two cations in a perovskite structure can be further analyzed with reference to the principles of crystal chemistry [15,16], where metallic ions always prefer to go into lattice sites with similar radii and equal valences. Considering the effect of ionic radii of the cations, the mechanism was analyzed using the fractional tolerance factor [15]. In this approach, the degrees of lattice

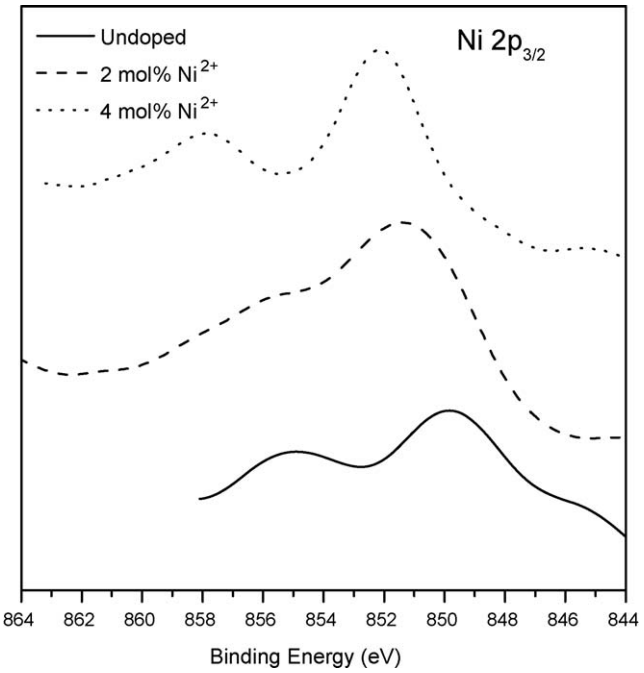

Fig. 1. XPS spectra for Nickel $2p_{3/2}$ of the undoped and Ni-doped ceramics sintered at 900 °C.

packing, t_1 and t_2, corresponding to A and B site ions in a perovskite lattice, are described by the following equations, respectively,

$$t_1 = \frac{\sqrt{2}(r_A + r_o)}{a} \quad (1)$$

$$t_2 = \frac{\sqrt{2}(r_B + r_o)}{a} \quad (2)$$

where a is the lattice parameter, r_A, r_B and r_o are the average ionic radii at A-sites, B-sites and ionic radius of the oxygen, respectively. If t_1 is less than 1 from the calculation, ions at A-site tend to fluctuate at higher mobility due to loose atomic packing at this specific site. Conversely, the perovskite unit cells are more closely packed at A-sites when the t_1 values are larger than 1. Similarly this concept is applicable to t_2 for ionic packing at B-sites.

Table 1 summarizes the calculated fractional tolerance factors for the doped and undoped compositions when Ni^{2+} and Mg^{2+} are assumed to enter either A or B site. The respective

Table 1
Calculated fractional tolerance factors based on different assumptions that the Ni^{2+} or Mg^{2+} ions substitutes either A or B-sites in a ABO_3 perovskite structure.

Composition	Lattice constant (Å)	Substitution solely at A-sites		Substitution solely at B-sites	
		t_1	t_2	t_1	t_2
Undoped	4.0365	1.0124	1.0189	1.0124	1.0189
2 mol% NiO	4.0365	1.0107			1.0192
4 mol% NiO	4.0365	1.0090			1.0195
1 mol% MgO	4.0365	1.0117			1.0190

ionic radii were determined with the corresponding coordination numbers in the perovskite unit cell [17–19]. From Table 1, t_1 and t_2 are greater than unity indicating all ions are closely packed in the perovskite crystal lattices. Based on the assumption that the excess Ni^{2+} enters only A-site, t_1 decreases and approaches 1 with excess Ni^{2+}, thus suggesting an increase in tendency for the ions to occupy A-site. However, t_2 increases based on the assumption that Ni^{2+} substitutes B-site, thus it is less likely to happen due to overcrowding. As a result, the substitution of cations in A-sites enhances perovskite phase stability as the fractional tolerance factor approaches unity under such an assumption. Similarly, this concept and conclusion apply for Mg^{2+} doping, according to the corresponding data of t_1 and t_2 given in Table 1.

Improved perovskite phase stability with the A-site substitutions of the doped compositions can further be supported by ionic charge consideration. If Ni^{2+} and Mg^{2+} enter B-sites to substitute the existing Ni^{2+}, Mg^{2+} and Zn^{2+}, insignificant difference to the perovskite structure is expected since all of them have similar radii and valences. On the other hand, it is also unlikely for the excess $Ni^{2+}$and Mg^{2+} to substitute Nb^{5+}, Ti^{4+} and Zr^{4+} of higher valences at B-sites because considerable oxygen vacancies would be created to maintain charge neutrality [15,20].

The enhanced perovskite stability when NiO or MgO were added to our complex compositions was confirmed by X-ray diffraction results. Figs. 2 and 3 present the XRD results of the ceramic disks sintered at different temperatures from 800 to 950 °C for undoped and 1 mol% Mg-doped samples, respectively. For the undoped sample sintered at 800 °C, in addition to the main perovskite phase, minor peaks corresponding to 2θ of 29.3°, 33.9°, 48.7° and 57.8° were also identified for the undesirable cubic pyrochlore phase, attributed to (2 2 2), (4 0 0), (4 4 0) and (6 2 2) reflections, respectively. With 1 mol% Mg-doping, the pyrochlore phase at 800 °C was significantly suppressed. However, with increasing the sintering temperatures above 850 °C, there was no detectable pyrochlore phase in all the ceramic disks.

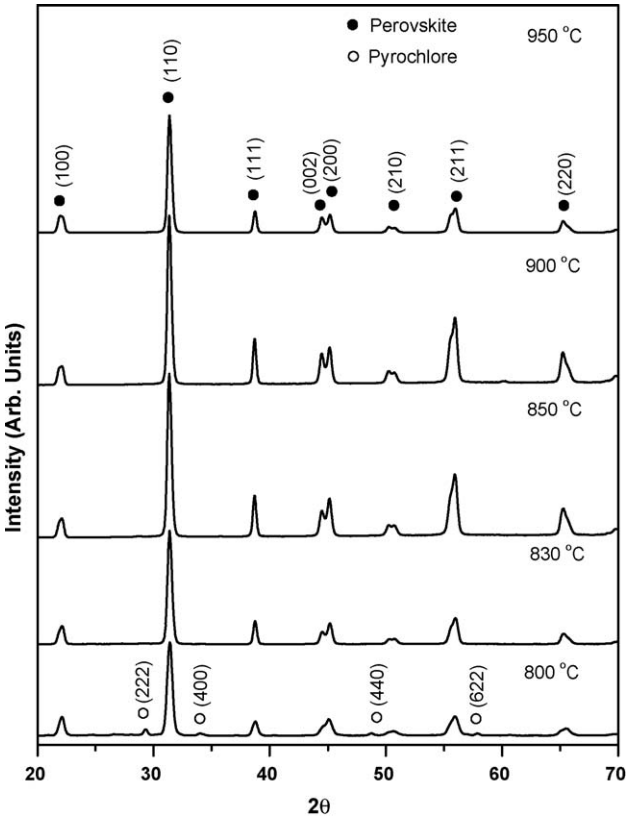

Fig. 2. XRD for the ceramics of undoped composition sintered at different temperatures from 800 to 950 °C for 1 h.

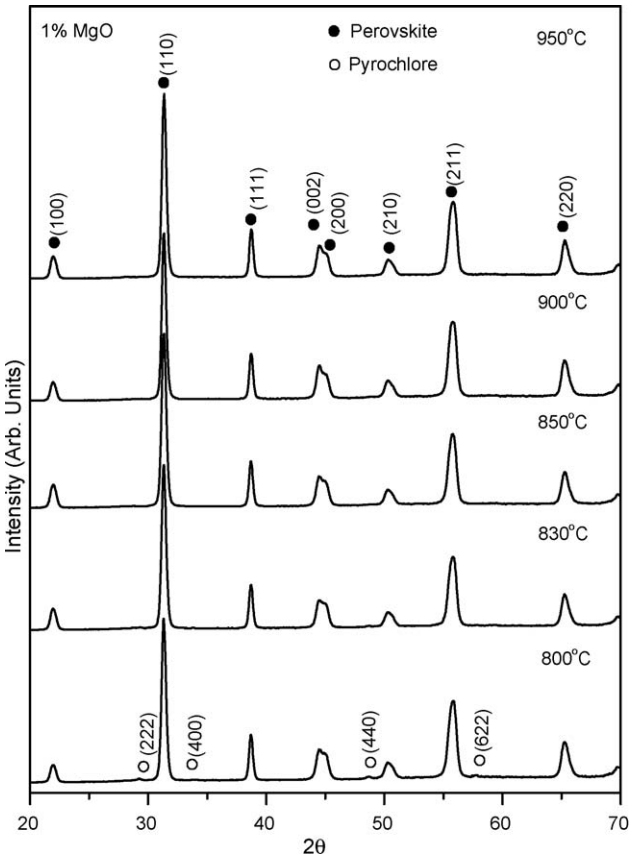

Fig. 3. XRD for the ceramics of the 1 mol% MgO doped composition sintered at different temperatures from 800 to 950 °C for 1 h.

From the XRD of the undoped composition as in Fig. 2, peak splitting at 44.9° and 45.1° (Fig. 2) was observed, corresponding to the (0 0 2) and (2 0 0) planes of a tetragonal structure. These two peaks became closer but still obviously separated with 2 mol% NiO (Fig. 4) or 1 mol% MgO (Fig. 3), while they were almost overlapped when doped with 4 mol% NiO (Fig. 5), indicating a reduction in tetragonality of the crystalline phase. Furthermore, this might also be an indication that both tetragonal and rhombohedral phases coexist as the structure shifts towards the rhombohedral phase with increasing the excess Ni^{2+}.

There are a few other studies suggesting various mechanisms for site-A substitutions in pervoskite phase [21,22]. However, these studies did not provide any experimental evidences about valence states as in this paper. Wakiya et al. [21] suggested that a cation with a smaller radius and similar

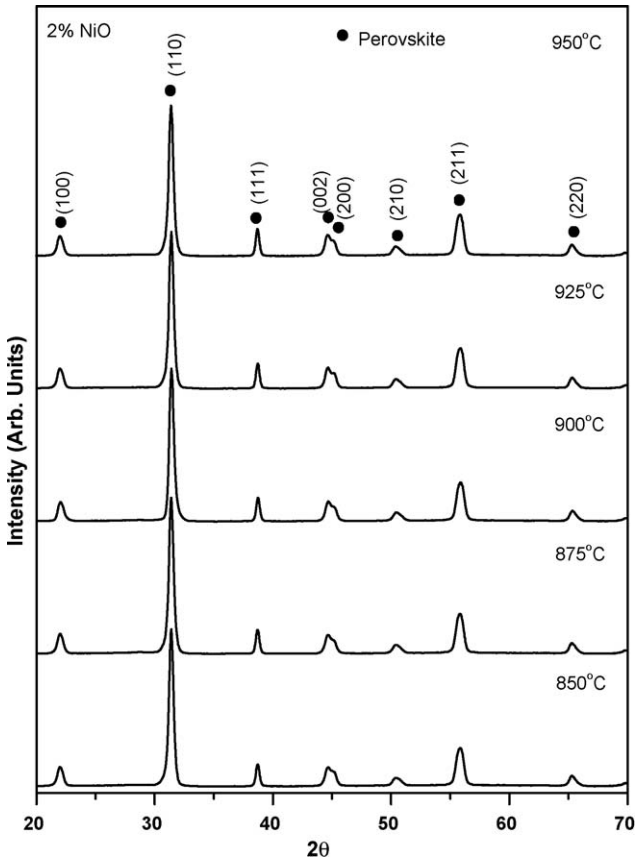

Fig. 4. XRD for the ceramics of 2 mol% NiO doped composition sintered at different temperatures from 850 to 950 °C for 1 h.

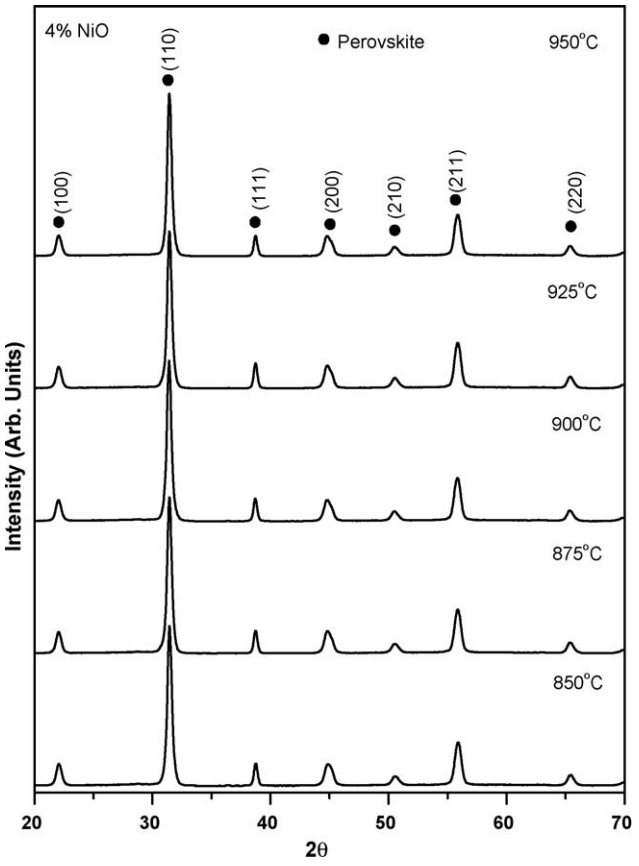

Fig. 5. XRD for the ceramics of the 4 mol% NiO doped composition sintered at different temperatures from 850 to 950 °C for 1 h.

valence can enhance the structure stability when substituting Pb^{2+} sites in a perovskite phase. Furthermore, it is believed that Ni^{2+} ($3d^8$) may lead to a more stable perovskite structure due to a possible overlapping of the empty d-orbital with the lone pairs of Pb^{2+}, thus is more effective in stabilizing the perovskite structure compared to Mg^{2+} ($3s^0$) doped composition. Goh et al. [22] found that bond valence approach could theoretically explain an enhanced stability of perovskite phase with excess Ni^{2+} in ferroelectric thin films based on the assumption that these cations enter the A-sites.

3.2. Sintered densities and morphologies

Fig. 6 shows the measured densities of ceramic disks for undoped and doped ceramics sintered at various temperatures. For the undoped composition, density was significantly increased with increasing sintering temperature, and the highest density of about 7.7 g/cm^3 was obtained at about 850 °C followed by slight drop with further increasing the temperature. For the NiO and MgO doped compositions, the density kept increasing with temperature increased up to 925 °C, and the highest densities obtained were about 7.9 g/cm^3 upon sintering above 900 °C. The error bars indicate discrepancies resulted from the density measurement using Archimedes principle.

Fig. 7(a)–(d) shows the morphology for the undoped and doped ceramics sintered at 950 °C. From these micrographs, grain sizes were reduced when doped with 2 mol% NiO and 1 mol% MgO. Larger grain sizes were observed with further addition of NiO content (4 mol%), as shown in Fig. 7(c). Small

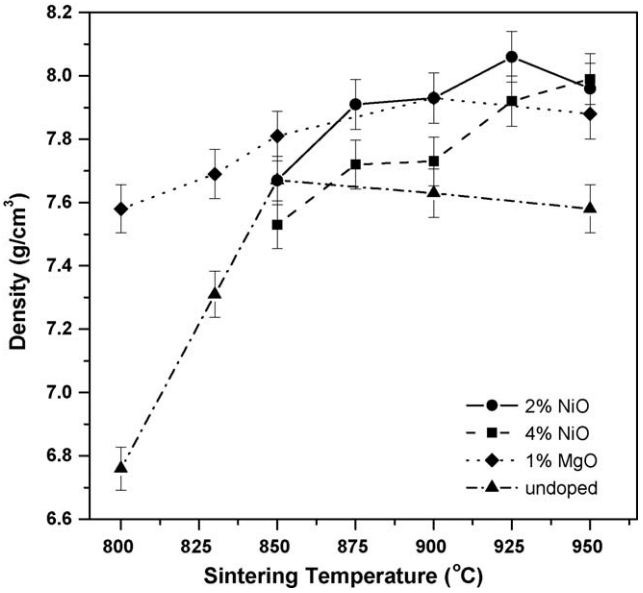

Fig. 6. Ceramic densities for doped and undoped compositions sintered at different temperatures from 800 to 950 °C.

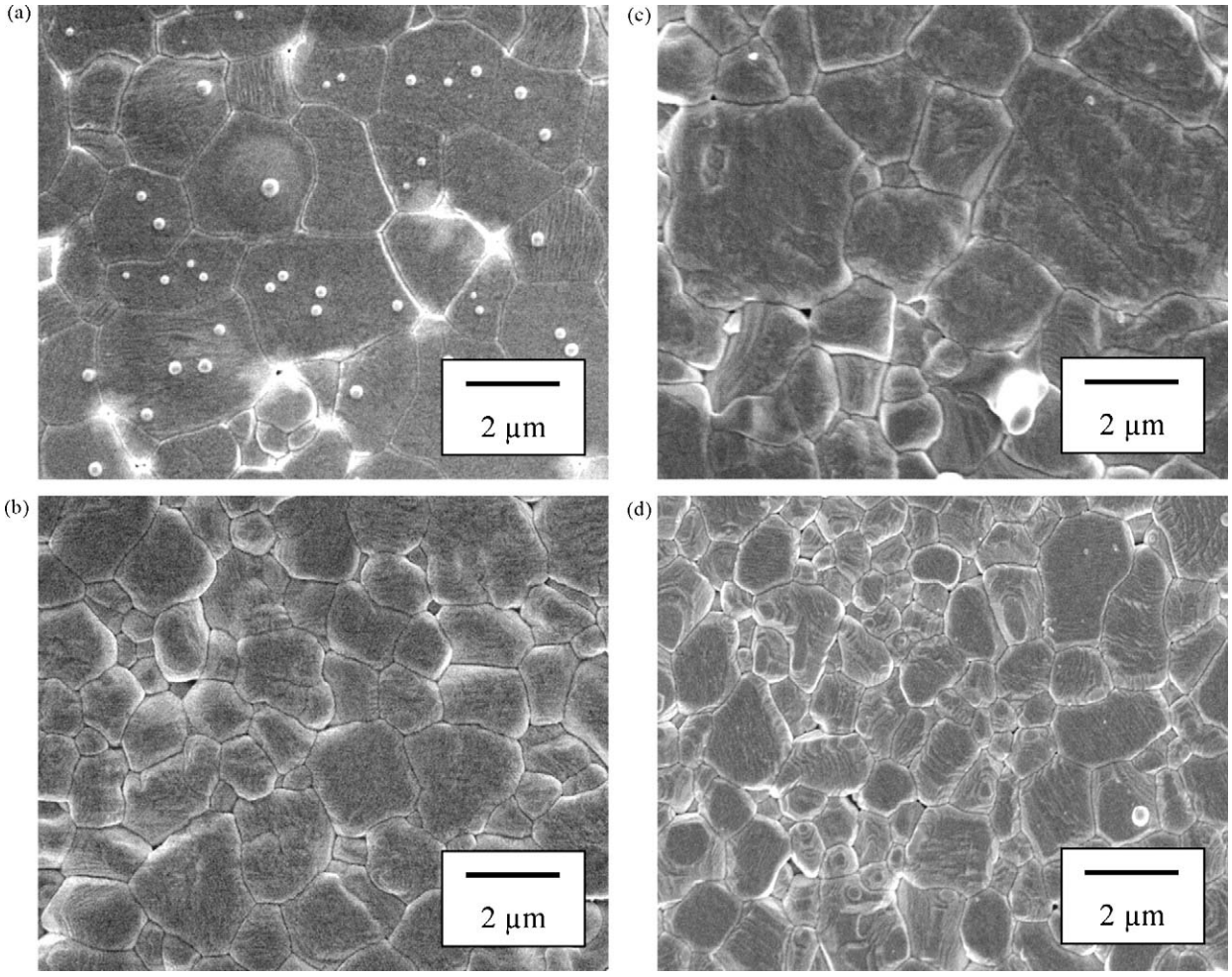

Fig. 7. SEM micrographs for the ceramics with (a) undoped composition, (b) 2 mol% NiO, (c) 4 mol% NiO and (d) 1 mol% MgO doped compositions, sintered at 950 °C after surface polishing and thermal etching.

round particles were found only in the undoped ceramics in Fig. 7(a), which were probably the secondary pyrochlore phase that was not detected from the XRD. The progressive densification for the 4 mol% NiO doped ceramics was shown in Fig. 8(a)–(c), with the sintering temperatures of 850, 900 and 925 °C, respectively, and in Fig. 7(c) for 950 °C. Considerably high densification was obtained at 925 °C in Fig. 8(c).

3.3. Electrical properties

The dielectric constant data for each composition sintered at various temperatures were summarized in Fig. 9. For the undoped composition, the dielectric constant increased with temperature and a large dielectric constant could only be obtained when sintered at 950 °C. However, when NiO and MgO were added, high dielectric constant above 2000 could be achieved at 850 °C. This result shows doping of NiO and MgO could substantially improve the dielectric constant at low sintering temperature, because the pyrochlore phase was eliminated to form single perovskite phase in the doped compositions. In addition, the dielectric loss for both the undoped and doped samples were low, in the range of 0.02–0.03 (not shown).

Fig. 10 presents typical hysteresis loops at 25 kV/cm for the undoped and doped compositions sintered at 900 °C. With an addition of NiO or MgO as dopants, significantly enhanced polarizations were obtained due to elimination of the pyrochlore phase. The composition with 4 mol% of NiO had the highest remnant polarization more than 20 μC/cm^2 with a lower coercive field. Fig. 11 shows piezoelectric coefficients d_{33} for the undoped and doped ceramics. Generally the piezoelectric coefficient increased with increasing sintering temperature from 800 to 900 °C. With an addition of 4 mol% NiO to the undoped composition, piezoelectric d_{33} was substantially improved over the undoped composition and reached 459 *pC/N* when sintered at 950 °C, which is a large piezoelectric coefficient among complex ceramic compositions with such a low sintering temperature [15,22].

The dielectric, ferroelectric and piezoelectric properties were all significantly enhanced with the doping of the MgO and NiO due to the enhanced stability of the perovskite structure and elimination of the pyrochlore phase. The reduction in

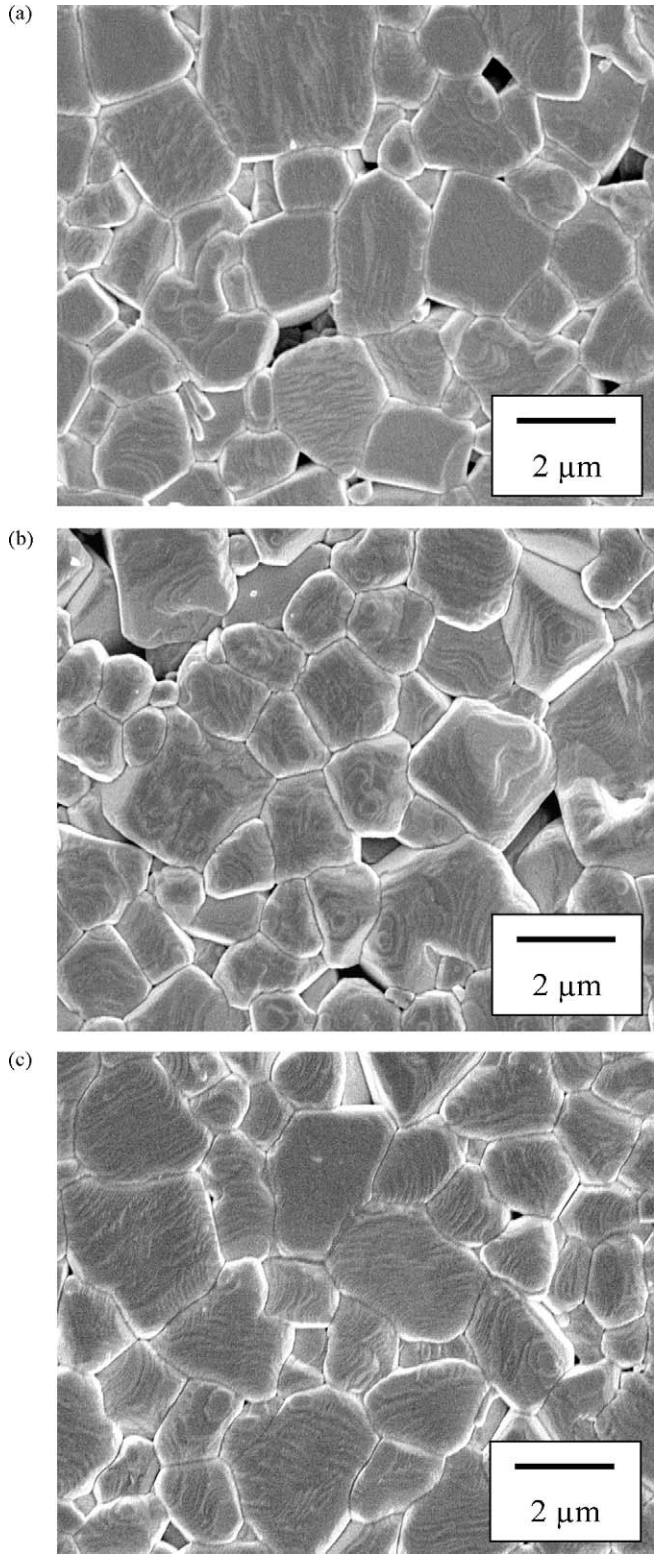

Fig. 8. SEM micrographs for 4 mol% NiO doped ceramics sintered at (a) 850 °C, (b) 900 °C, and (c) 925 °C, after surface polishing and thermal etching.

tetragonality of the perovskite phase in the doped compositions, indicating structural shift towards the MPB, may also contribute to the improved properties. A possible coexistence of both rhombohedral and tetragonal structures might happen

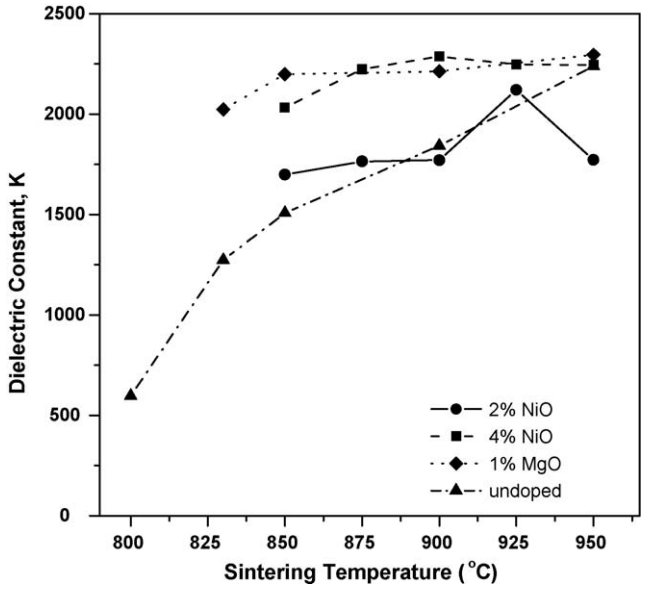

Fig. 9. Dielectric constant at room temperature at 1 kHz for undoped and doped compositions sintered at various temperatures from 800 to 950 °C.

near the 4 mol% NiO-doped composition. The reduced tetragonality can enhance the ferroelectric and piezoelectric properties due to the improved mobility of domain walls and polarization switching. This is also consistent with the lower coercive field as observed for the 4 mol% NiO-doped composition as shown in Fig. 10. Shift of T_c to lower temperature by the small amount of doping was not significant here and it is believed that this did not substantially contribute to the change of the properties. That is one of the reasons for that the enhancements in both dielectric constant and ferroelectric polarization were observed at room temperature with the doping.

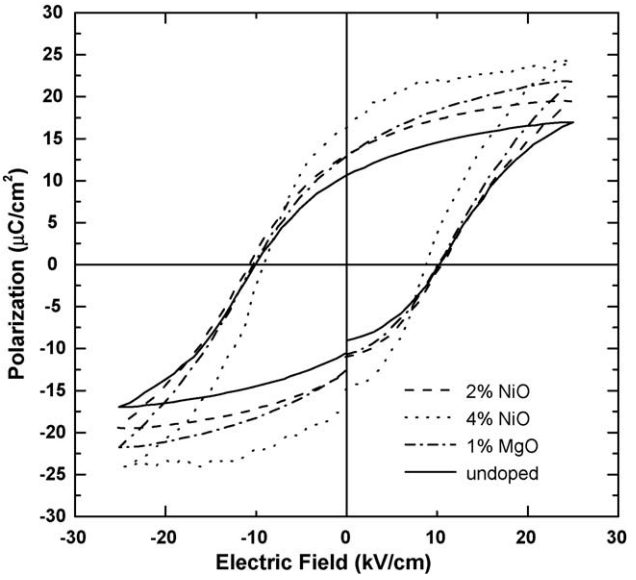

Fig. 10. Polarization–electric field (*P–E*) hysterisis loops for undoped and doped compositions sintered at 900 °C.

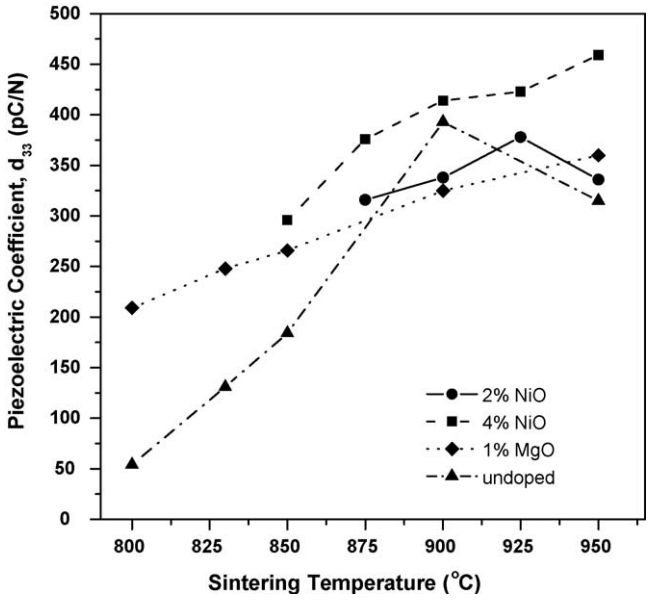

Fig. 11. Piezoelectric coefficient d_{33} at 110 Hz for the undoped and doped compositions sintered at various temperatures from 800 to 950 °C.

4. Conclusions

Excess valence-two cations, Ni^{2+} and Mg^{2+}, were introduced to a ferroelectric perovskite ceramic with a complex composition (0.10PNN–0.35PZN–0.15PMN–0.10PZ–0.30PT) to promote the perovskite phase while suppress the pyrochlore phase. Both XPS experimental results and theoretical analyses on the basis of ionic packing indicate the excess valence-two ions substituting the A-sites in the ABO_3 perovskite structure. With the enhanced perovskite phase and densification with excess NiO and MgO, improved piezoelectric coefficient d_{33} up to 459 *pC/N*, higher ferroelectric remnant polarization and dielectric constant were demonstrated when sintered at temperature as low as 850–950 °C.

Acknowledgements

The authors thank Mr Xujiang He, Dr Shuhui Yu, and Ms Phoi Chin Goh for their assistances and helpful discussions. The supports from the ceramics group, Materials Science Department in National University of Singapore are also acknowledged.

References

[1] T.R. Shrout, A. Halliyal, Preparation of lead-based ferroelectric relaxors for capacitors, Am. Ceram. Soc. Bull. 66 (1987) 704–711.
[2] C. Miclea, C. Tanasoiu, C.F. Miclea, L. Amarande, A. Gheorghiu, F.N. Sima, Effect of iron and nickel substitution on the piezoelectric properties of PZT type ceramics, J. Eur. Ceram. Soc. 25 (2005) 2397–2400.
[3] H. Fan, H.E. Kim, Perovskite stabilization and electromechanical properties of polycrystalline lead zinc niobate-lead zirconate titanate, J. Appl. Phys. 91 (2002) 317–322.
[4] B.K. Gan, K. Yao, X.J. He, Complex oxide ferroelectric ceramics $Pb(Ni_{1/3}Nb_{2/3})O_3$–$Pb(Zn_{1/3}Nb_{2/3})O_3$–$Pb(Mg_{1/3}Nb_{2/3})O_3$–$PbZrO_3$–$PbTiO_3$ with low sintering temperature, J. Am. Ceram. Soc. 90 (2007) 1186–1192.
[5] K. Shiratsuyu, K. Hayashi, A. Ando, Y. Sakabe, Piezoelectric characterization of low-temperature-fire $Pb(Zr, Ti)O_3$–$Pb(Ni, Nb)O_3$ ceramics, Jpn. J. Appl. Phys. 39 (2000) 5609–5612.
[6] E. Goo, T. Yamamoto, K. Okazaki, Microstructure of lead-magnesium niobate ceramics, J. Am. Ceram. Soc. 69 (1986) C188–C190.
[7] U. Syamaprasad, A.R. Sheejanair, M.S. Sarma, P. Guruswamy, P.S. Mukherjee, A.D. Damodaran, L. Krishnamurthy, M. Achuthan, Multilayer capacitor ceramics in the PMN-PT-BT system: effect of MgO and $4PbO{\cdot}B_2O_3$ additions, J. Mater. Sci.: Mater. Electron. 8 (1997) 199–205.
[8] X. Wan, X. Tang, J. Wang, H.L.W. Chan, C.L. Choy, Cationic ordering structures of lead magnesium niobates with isovalent dopants having different ionic radii, Jpn. J. Appl. Phys. 37 (1998) 5249–5252.
[9] X. Wan, X. Tang, J. Wang, H.L.W. Chan, C.L. Choy, Growth and pyroelectric property of 0.2 mol% Fe-doped $Pb(Mg_{1/3}Nb_{2/3})O_3$–$0.38PbTiO_3$ single crystals measured by a dynamic technique, Appl. Phys. Lett. 84 (2004) 4711–4713.
[10] Y.M. Lu, W.S. Hwang, J.S. Yang, Effects of substrate temperature on the resistivity of non-stoichiometric sputtered NiO_x films, Surf. Coat. Technol. 155 (2002) 231–235.
[11] M.A. Van Veenendaal, G.A. Sawatzky, Nonlocal screening effects in 2p X-ray photoemission spectroscopy core-level line shapers of transition metal compounds, Phys. Rev. Lett. 70 (1993) 2459–2462.
[12] V. Biju, M. Abdul Khadar, Electronic structure of nanostructured nickel oxide using Ni 2p XPS analysis, J. Nanoparticle Res. 4 (2002) 247–253.
[13] M. Stojanovic, R.G. Haverkamp, C.A. Mims, H. Moudallal, A.J. Jacobson, Synthesis and characterization of $LaCr_{1-x}Ni_xO_3$ perovskite oxide catalysts, J. Catal. 165 (1997) 315–323.
[14] N. Ohtsu, M. Oku, T. Shishido, K. Wagatsuma, X-ray photoelectron spectroscopic studies on phase identification and quantification of nickel aluminides, Appl. Surf. Sci. 253 (2007) 8713–8717.
[15] A. Tkach, P.M. Vilarinho, A. Kholkin, Effect of Mg doping on the structural and dielectric properties of strontium titanate ceramics, Appl. Phys. A 29 (2004) 2013–2020.
[16] M. Ghita, M. Fornari, D.J. Singh, S.V. Halilov, Interplay between A-site and B-site driven instabilities in perovskites, Phys. Rev. B72 (2005) 054114.
[17] N. Wakiya, K. Shinozaki, N. Mizutani, Estimation of phase stability in $Pb(Mg_{1/3}Nb_{2/3})O_3$ and $Pb(Zn_{1/3}Nb_{2/3})O_3$ using the bond valence approach, J. Am. Ceram. Soc. 80 (1997) 3217–3220.
[18] S.S. Batsonov, A systematic presentation of atomic radii, J. Struct. Chem. 3 (5) (1962) 590–603.
[19] R.D. Shannon, C.T. Prewitt, Effective ionic radii in oxides and fluorides, Acta Cryst. B25 (1969) 925–946.
[20] A. Molak, E. Talk, M. Kruczek, M. Paluch, A. Ratuszna, Z. Ujma, Characterisation of $Pb(Mn_{1/3}Nb_{2/3})O_3$ by SEM, XRD, XPS and dielectric permittivity tests, Mater. Sci. Eng. B128 (2006) 16–24.
[21] N. Wakiya, N. Ishizawa, K. Shinokaki, N. Mizutani, Thermal stability of $Pb(Zn_{1/3}Nb_{2/3})O_3$ (PZN) and consideration of stabilization conditions of perovskite type compounds, Mater. Res. Bull. 30 (1995) 1121–1131.
[22] P.C. Goh, K. Yao, Z. Chen, Ferroelectric thin films with complex composition of PNN–PZN–PMN–PZ–PT and excess NiO, J. Mater. Res. 23 (2) (2008) 536–542.